J Mater Sci (2007) 42:3778–3782
DOI 10.1007/s10853-006-0411-2

# Observation of an ultraviolet emission band in $TiO_2$ nanocrystals doped with $Eu^{3+}$

**Q. G. Zeng · Z. J. Ding · Z. M. Zhang**

Received: 10 November 2005 / Accepted: 5 May 2006 / Published online: 11 February 2007

**Abstract** The photoluminescence spectra of titanium dioxide ($TiO_2$) nanocrystals doped with $Eu^{3+}$ (molar ratio $Eu^{3+}/TiO_2$ = 0, 1, 2, 4%) are investigated under different excitation wavelengths. An ultraviolet band of emission energy higher than the energy gap is found for excitation wavelengths larger than 315 nm when the $Eu^{3+}$ content is higher than 2%. The new emission band redshifts and its emission intensity is intensified with the increase of excitation wavelength. The emission mechanism for the new ultraviolet emission band is analyzed.

## Introduction

In recent years, titanium dioxide ($TiO_2$) nanocrystal has attracted much attention because of its potential applications in photo-electrochemical solar cells, photocatalysis, and optical coating [1, 2]. The photoluminescence (PL) of the bulk $TiO_2$ cannot be observed at room temperature due to its indirect transition nature. However, for nano-$TiO_2$ the surface state is a major factor influencing the emission of exciton. The surface states, such as surface trapped state [3], defect state, and oxygen vacancy [4], can form the emission centers. Therefore, some emission bands of the $TiO_2$ nanocrystal have been observed at room temperature recently. Two emission peaks at 382 nm and 420 nm have been observed from the nano-sized $TiO_2$ colloids by Liu et al. [5] (the particle size ranges from 2 nm to 4 nm) and are attributed to band to band transition. Hirendra et al. observed the emission at 450 nm from $TiO_2$ nanoparticles (about 2–4 nm) in microemulsion solutions [3]. A 390 nm emission band associated with framework Ti in mesoporous titanosilicates was observed by Avelino et al. [6]. Tang et al. [7] have studied the luminescence in visible light range varied with temperatures for anatase $TiO_2$ and doped $TiO_2$. The previous studies on $TiO_2$ [3–7] have a common feature that the emission energy is smaller the energy gap 3.2~3.3 eV. But very few literatures have reported ultraviolet emission band (the corresponding energy is higher than energy gap) for the anatase $TiO_2$ nanocrystals.

In this work, $TiO_2$ nanocrystals doped with $Eu^{3+}$ ($Eu^{3+}/TiO_2$ nanocrystals) are synthesized by the sol–gel method with hydrothermal treatment. These nanocrystals powders are characterized by means of transmission electron microscope (TEM), X-ray diffraction (XRD) and UV–vis. absorption spectrum. We also measure PL spectra of the nanocrystals with different excitation wavelengths.

## Experimental

At room temperature, $Eu_2O_3$ and nitric acid are added to the deionized water with pH = 2, which is vigorously

Q. G. Zeng (✉) · Z. J. Ding · Z. M. Zhang
Hefei National Laboratory for Physical Sciences
at Microscale and Department of Physics, University
of Science and Technology of China, Hefei, Anhui 230026,
P.R. China
e-mail: zengqg@mail.ustc.edu.cn

Q. G. Zeng
Department of Mathematics and Physics, Wu Yi University,
Jiangmen, Guangdong 529020, P.R. China

stirred. After half an hour, tetrabutyl titanate, $Ti(OC_4H_9)_4$, is slowly dripped into above solution also with vigorously stirring for 1 h, and then the solution is heated to 353 K. The mixture is obtained after 10 h, followed by hydrothermal treatment in the autoclave at 500 K for 12 h. The resulting gel is repeatedly washed with ethanol and then annealed in air for 6 h at 773 K. The average sizes are, respectively, about 23.5 nm and 13.2 nm estimated from TEM micrographs for the $Eu^{3+}/TiO_2$ molar ratio of 0% and 2%.

The structural studies of $Eu^{3+}/TiO_2$ nanocrystals are performed on a X-ray diffractometer (X'PERT PRO, PHILIPS) with a monochromatized source of Cu-K$\alpha_1$ radiation at wavelength of 0.15405 nm. The transmission electron micrographs are obtained by using a TEM (H-800). The steady-sate/lifetime spectrofluorometer (FLUORLOG–3-TAU, JY) is used to record PL spectra at room temperature by the excitation wavelength of 275, 300, 315, 320, 325 and 330 nm, respectively, with 450-W xenon lamp. The PL spectra are corrected by a standard curve for the spectral response of the detector.

## Results

The XRD patterns for samples of the different molar ratios of $Eu^{3+}/TiO_2$ ($Eu^{3+}\% = 0, 1, 2, 3, 4$) are given in Fig. 1, which show that the crystal form of the nanocrystals is anatase. Lattice parameters are calculated to determine whether the $Eu^{3+}$ could enter into the $TiO_2$ lattice resulting in the formation of solid solutions [8]. Considering the relatively large difference in the ion radii of $Eu^{3+}$ (0.68 A) and $Ti^{4+}$ (0.95 A), which indicate that the $Eu^{3+}$ ions cannot enter the $TiO_2$ lattice because the $TiO_2$ lattice parameter should be enlarged if the $Eu^{3+}$ ions entered into the $TiO_2$ lattice. In addition, it is found the Eu–O–Ti bonds from XPS spectrum (not shown) for the $Eu^{3+}/TiO_2$ nanocrystals. Therefore, we consider the Eu–O–Ti bonds are formed on the surface of the $TiO_2$ lattice.

The PL spectra inss Fig. 2 are recorded by the steady-sate/lifetime spectrofluorometer (FLUORLOG–3-TAU, JY. Co.) and are measured for different excitation wavelengths by xenon lamp at room temperature. It is observed from Fig. 2, the PL spectra of the $Eu^{3+}/TiO_2$ nanocrystals, that the peaks at 392 nm and 425 nm have no any position shift with the increase of excitation wavelength. These two peaks relate to the self-trapped state and defect-trapped state [3–7]. However, for excitation wavelength larger than 315 nm, a new ultraviolet emission band centered at 357 nm (3.48 eV) appears for the $Eu^{3+}$ content higher than 2%. Furthermore, this emission band redshifts and the emission intensity dramatically increases with excitation wavelength. To the best of our knowledge, this is the first observation of the band in $Eu^{3+}/TiO_2$ nanocrystals. It should be noted that this emission band is not obvious in pure $TiO_2$ nanocrystal at the same excitation wavelengths.

The UV–vis. spectroscopy is used to obtain the extinction of the $Eu^{3+}/TiO_2$ nanocrystals for $Eu^{3+}$

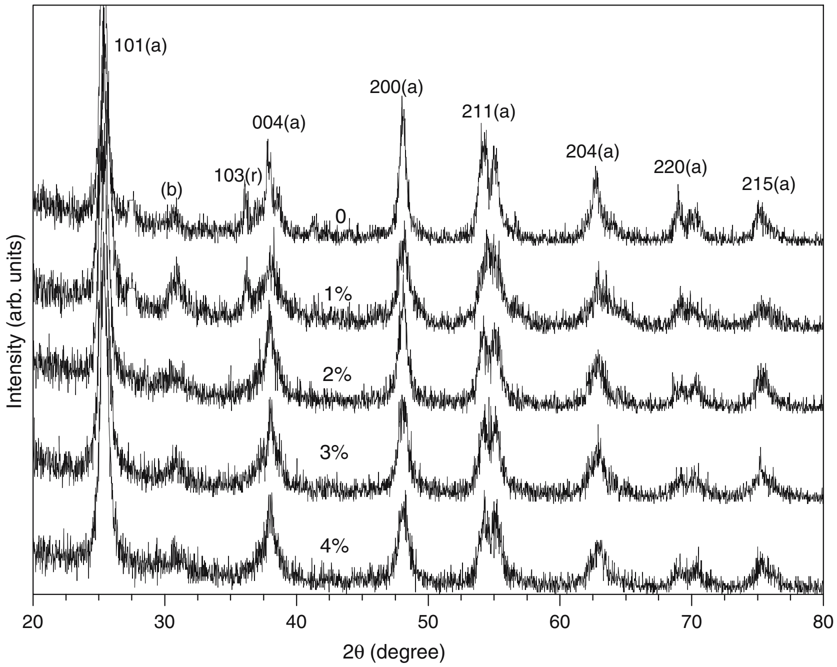

**Fig. 1** XRD pattern of the $Eu^{3+}/TiO_2$ nanocrystals (the $Eu^{3+}$ concentration, i.e., molar ratio in the samples, are 0, 1, 2, 3 and 4%, respectively). The letters a, r and b represent the crystalline forms anatase, rutile and brookite, respectively

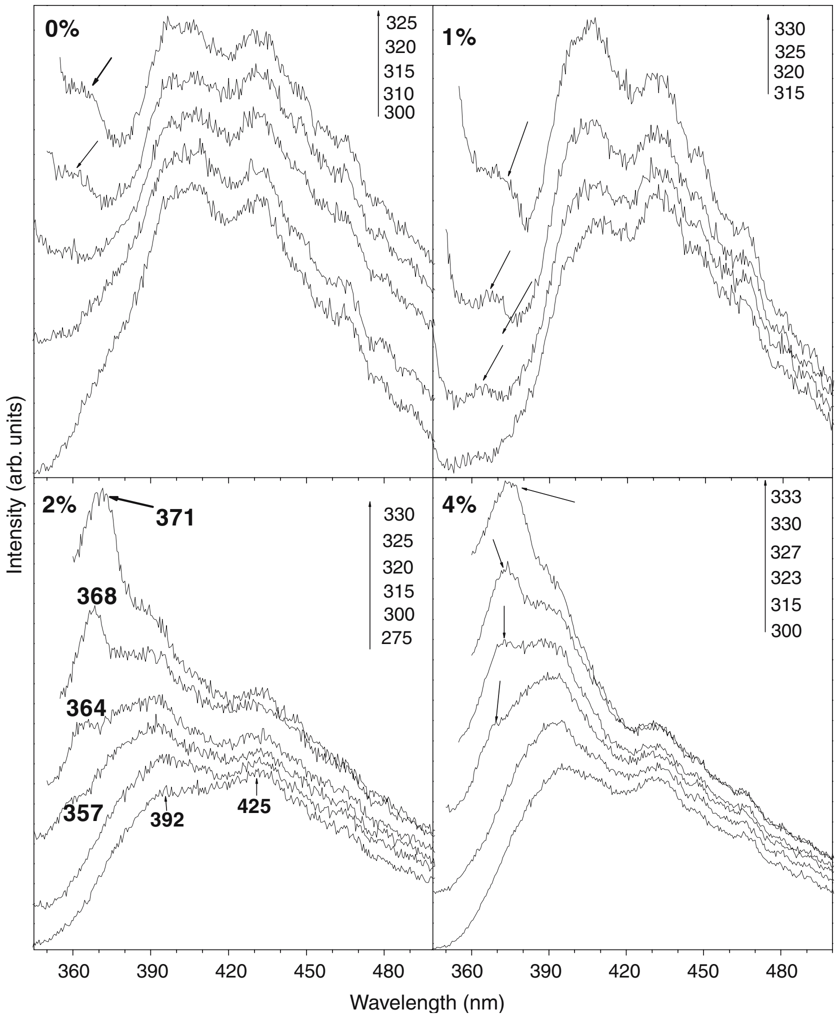

**Fig. 2** The PL spectra measured for $Eu^{3+}/TiO_2$ ($Eu^{3+}\% = 2\%$) nanocrystals at different excitation wavelengths of 275, 300, 315, 320, 325 and 330 nm, respectively. The wavelength at 357 nm, 364 nm, 368 nm and 371 nm is the center position of the new band

concentrations of 0% and 2% in Fig. 3. The absorption edge is blueshifted for the sample ($Eu^{3+}/TiO_2 = 2\%$) due to the grain size effect [9, 10]. This result is consistant with the TEM observation of the nanocrystals in Fig. 4. For $Eu^{3+}$ it has no crystal field absorption transition at 330 nm [11]. We have also measured UV–vis. transmission spectra of the $Eu^{3+}/TiO_2$ nanocrystals for different $Eu^{3+}$ concerntration ($Eu^{3+}/TiO_2 = 0, 1, 2, 3, 4\%$) in ethanol solution; but the absorption peak of $Eu^{3+}$ was not detected at any case. Therefore, the ultraviolet emission band is origined from $TiO_2$ but not from the $Eu^{3+}$. Because the energy of the emission band (3.48 eV) is larger than the absorption edge (3.2 eV) of the $Eu^{3+}/TiO_2$ nanocrystal samples, the excitation state of the emission band may lie inside conduction band.

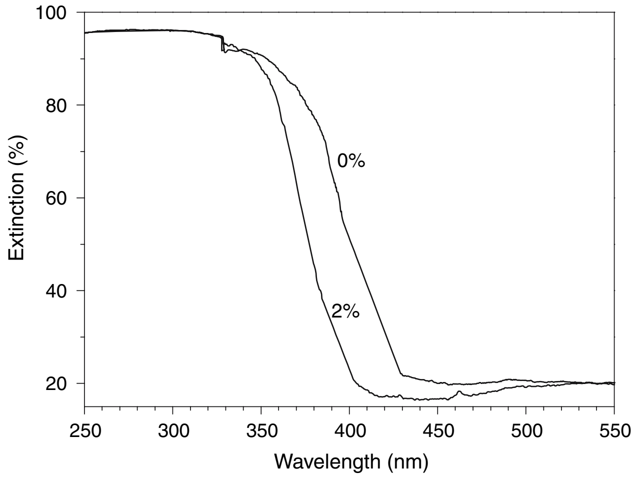

**Fig. 3** The UV–vis. spectroscopy measured extinction of the $Eu^{3+}/TiO_2$ nanocrystals for $Eu^{3+}$ concentrations of 0% and 2%

## Discussion

The band gap of $TiO_2$ nanocrystal is estimated to be 3.2 eV from Fig. 3, which is less than the energy of 3.48 eV, the photon energy of the new emission band

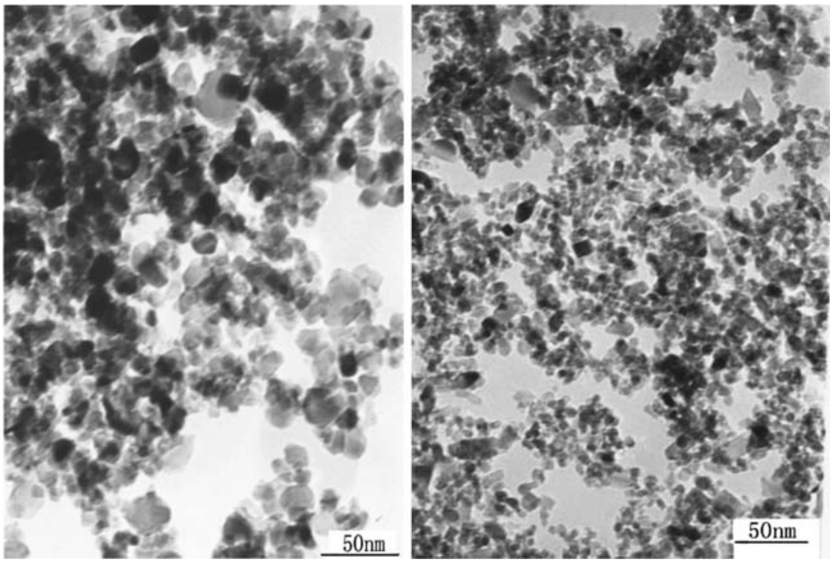

**Fig. 4** TEM images of the $TiO_2$ (left) nanocrystals and $Eu^{3+}/TiO_2$ ($Eu^{3+}\% = 2\%$) nanocrystals (right)

at 357 nm. Theoretical calculations [12, 13] show that there are discrete conduction bands (or subconduction bands) in $TiO_2$ crystal, especially for smaller dimensional particles [14]. Therefore, it is reasonable to consider that the new ultraviolet emission band may be caused by carrier recombination from the discrete conduction bands (or subconduction bands) to valence band [15]. For the none or low content of $Eu^{3+}$ (less than 2%) doped in $TiO_2$ nanocrystals, the carriers can across easily the lattice and nonradiatively recombine or diffuse to neighboring luminescent centers. But for the higher content of $Eu^{3+}$, the Eu–O–Ti bonds formed on the surface of the $TiO_2$ lattice can act as an energy barrier to prevent carrier tunneling through it [15]. As a result the carriers are located in $TiO_2$ lattice, indicating that the $TiO_2$ nanocrystals can be passivated by the $Eu^{3+}$. The similar results have also been found in the Mn or Fe passivated porous silicon [15, 16].

The above analysis leads to the explanation of the experimental results as follows: In the case of higher content of $Eu^{3+}$ (>2%), the smaller excitation energy is, the more carriers are prevented tunnelling from $TiO_2$ nanocrystals to neighboring defect states (as shown in Fig. 5) for recombination due to the existence of Eu–O–Ti on the surface of the $TiO_2$ nanocrystals. Therefore, the carrier recombination from conduction band (subconduction band or discrete level in conduction band) to valence band is enhanced, resulting in an increased intensity of the new ultraviolet emission band with the increase of the excitation wavelength in Fig. 2. In addition, the particle sizes (shown in Fig. 4) introduce a distribution of the energy gap by the quantum confinement effect. The variation of the excitation wavelength or the excitation photon energy is not able to create nonequilibrium carriers across the band gap of the small crystal [15]. The emission energy then shifts to the lower energy side or the emission wavelength redshifts with the excitation wavelength.

The electronic band structure of $TiO_2$ was calculated in Refs. [12, 13]. It was found that the allowed transitions of the lowest energy are indirect transitions from the edge to the center of the Brillouin zone (BZ), namely, $\Gamma_{1b} \rightarrow X_{1a}$ (2.91 eV with $\overrightarrow{E} \perp \overrightarrow{C}$) and $X_{1b} \rightarrow \Gamma_3$ (3.18 eV with $\overrightarrow{E} || \overrightarrow{C}$). In addition, the first direct-allowed transitions are at the $X$ edge of the BZ; $X_{1b} \rightarrow X_{1a}$ (3.45 eV with $\overrightarrow{E} \perp \overrightarrow{C}$) and $X_{1b} \rightarrow X_{2b}$ (3.59 eV with $\overrightarrow{E} || \overrightarrow{C}$), respectively [13, 14]. Here, we give a possible assignment for these emission peaks as follows: The emission peaks at 392 nm (3.16 eV) and 425 nm (2.92 eV) are assigned to the indirect transitions $X_{1b} \rightarrow \Gamma_3$ and $\Gamma_{1b} \rightarrow X_{1a}$, respectively. Whereas the center position of the new emission band ranged from 356 nm (3.48 eV) to 371 nm (3.35 eV) at different excitation wavelengths in Fig. 2 can be assigned to direct transitions $X_{1b} \rightarrow X_{1a}$ or $X_{2b}$. The

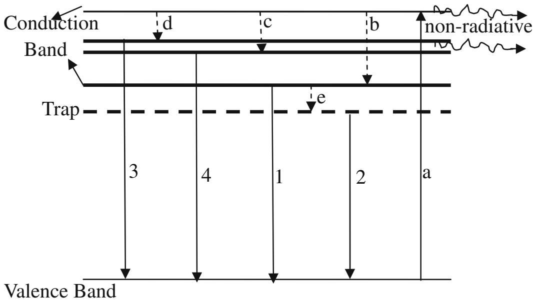

**Fig. 5** The scheme of the transitions between energy levels

detailed emission process is schematically drawn in Fig. 5. The pathways 1 and 2 represent the emission peaks at 392 nm and 425 nm, respectively, while the pathways 3 or 4 correspond to the new emission band.

## Conclusion

For the excitation wavelength longer than 315 nm an ultraviolet emission band is observed for the $TiO_2$ doped with the $Eu^{3+}$. The photon energy of the emission band is higher than the energy gap of the $TiO_2$. With the increase of excitation wavelength, the emission band redshifts and the intensity is enhanced; this is due to the Eu–Ti–O on the surface of the $TiO_2$ lattice preventing the carriers tunnelling from $TiO_2$ lattice to neighboring defect states for recombination.

**Acknowledgements** This work was supported by the National Natural Science Foundation of China (Grant No. 10574121 and 10025420), Natural Science Foundation of Anhui Province of China (Grant No. 05021015), Chinese Education Ministry and Chinese Academy of Sciences.

## References

1. Linsebigler AL, Lu G, Yates JT Jr (1995) Chem Rev 95:735
2. Ting CC, Chen SY, Hsieh WF, Lee HY (2001) J Appl Phys 90:5564
3. Hirendra NG, Soumyakanti A (2001) Langmuir 17:4129
4. Gu F, Wang SF, Song CF, Lv MK, Qi YX, Zhou GJ, Xu D, Yuan DR (2003) Chem Phys Lett 372:451
5. Liu Y, Claus RO (1997) J Am Chem Soc 119:5273
6. Avelino C, Hermenegildo G, Maria TN, Emilio JP, Fernando R (2000) Chem Mater 12:3068
7. Tang H, Berger H, Schmid PE, Levy F, Burri G (1993) Solid State Commun 87:847
8. Lin J, Yu JC (1998) J Photochem Photobio A: Chem 116:63
9. Zhang WF, Zhang MS, Yin Z, Chen Q (2000) Appl Phys B 70:261
10. Harish P, Anjiana D, Raghunandan B, Roland AF (2002) J Mater Chem 12:1625
11. Frindell KL, Bartl MH, Popitsch A, Stucky GD (2002) Angew Chem 114:1001
12. Asahi R, Taga Y, Mannstadt W, Freeman AJ (2000) Phys Rev B 61:7459
13. Daude N, Gout C, Jouanin C (1977) Phys Rev B 15:3229
14. Serpone N, Lawless D, Khairutdinov R (1995) J Phys Chem 99:16646
15. Chen QW, Zhu DL, Zhang YH (2000) Appl Phys Lett 77:854
16. Chen QW, Li X, Zhang Y (2001) Chem Phys Lett 343:507